

Spatial random field models based on Lévy indicator convolutions

Thomas Opitz¹

April 6, 2024

Abstract

Process convolutions yield random fields with flexible marginal distributions and dependence beyond Gaussianity, but statistical inference is often hampered by a lack of closed-form marginal distributions, and simulation-based inference may be prohibitively computer-intensive. We here remedy such issues through a class of process convolutions based on smoothing a $(d+1)$ -dimensional Lévy basis with an indicator function kernel to construct a d -dimensional convolution process. Indicator kernels ensure univariate distributions in the Lévy basis family, which provides a sound basis for interpretation, parametric modeling and statistical estimation. We propose a class of isotropic stationary convolution processes constructed through hypograph indicator sets defined as the space between the curve $(s, H(s))$ of a spherical probability density function H and the plane $(s, 0)$. If H is radially decreasing, the covariance is expressed through the univariate distribution function of H . The bivariate joint tail behavior in such convolution processes is studied in detail. Simulation and modeling extensions beyond isotropic stationary spatial models are discussed, including latent process models. For statistical inference of parametric models, we develop pairwise likelihood techniques and illustrate these on spatially indexed weed counts in the Bjertop data set, and on daily wind speed maxima observed over 30 stations in the Netherlands.

Keywords: composite likelihood; covariance function; extremal dependence; kernel convolution; Lévy basis; non-Gaussian geostatistics

¹BioSP, INRA, 84914, Avignon, France. E-mail: Thomas.Opitz@inra.fr

1 Introduction

Gaussian processes are widely used in spatial statistics thanks to their nice theoretical and statistical properties, but they may present critical shortcomings when features such as non-Gaussian marginal distributions, asymmetry in univariate and multivariate lower and upper tails or relatively strong dependence at extremal levels are crucial when modeling data. Some of these shortcomings may be remedied by applying marginal transformations or by embedding a random variable for the mean or the scale of the process (e.g., [Røislien and Omre, 2006](#); [Krupskii et al., 2017](#); [Huser et al., 2017](#)), but then statistical inference may become more challenging, and the model may not be identifiable if spatial data are not replicated in time. Hierarchical models including unobserved Gaussian components have become popular with Bayesian inference approximating the posterior distribution (e.g., [Rue et al., 2009](#); [Banerjee et al., 2014](#)), but we often lack closed-form distribution functions and densities. Moreover, such models often rely on conditional independence assumptions with respect to latent components, leading to dependence strength that is even weaker than the Gaussian one. Spatial copula approaches ([Joe, 2014](#)) propagate a full separation of marginal distributions and of dependence in spatial data. This leads to considerable flexibility, but then interpreting covariance structure becomes less intuitive, inference may be tricky when some parameters influence both margins and dependence, and one may view this as abandoning to seek modeling of the true data generating mechanism ([Mikosch, 2006](#)).

To remedy such modeling issues, process convolution methods have been proposed as a powerful alternative to generate models for stochastic processes with flexible and complex dependence structures (e.g., [Higdon, 1998](#); [Brix, 1999](#); [Higdon, 2002](#); [Hellmund et al., 2008](#); [Calder, 2008](#)). However, in practice, most approaches focus on Gaussian processes, whose convenient stability properties preserves multivariate Gaussian distributions in the convolution process. Non-Gaussian source processes have been used (e.g., [Kozubowski et al., 2013](#); [Jónsdóttir et al., 2013](#); [Barndorff-Nielsen et al., 2014](#); [Bousset et al., 2015](#); [Noven et al., 2015](#)), but they are often restricted to simulation-based inference to remedy the absence of closed-form expressions for marginal distributions, whose interpretation also becomes less intuitive. In contrast, our aim here is to develop a general non-Bayesian framework of spatial process convolution models with flexible and easily interpretable marginal distributions and dependence structures, amenable to inference based on covariograms or composite likelihoods.

The general idea of kernel convolutions is to smooth a random measure $L(\cdot)$ through a nonnegative kernel k to generate the convolution process $X(s) = \int k(s, y)L(dy)$. The source measure L assigns measure $L(A) = \int_A L(ds)$ to bounded Borel sets A . For the source process L to behave like white noise over continuous space, it must be a *Lévy process* characterized by independent increments ([Sato, 1999](#); [Barndorff-Nielsen et al., 2012](#)), and the collection of random variables $L(A)$ for arbitrary sets A is called a *Lévy basis*. The random variables $L(A)$ have infinitely divisible distribution, for instance the stable distributions (Gaussian, Cauchy, ...) or the gamma, inverse

Gaussian, compound Poisson, Poisson or negative binomial distributions. Conversely, to construct a white noise source process over continuous space, we may fix an infinitely divisible distribution F_A for the random measure $L(A)$ of a fixed bounded Borel set A , and thanks to the infinitely divisible structure we can then define a stationary and isotropic white noise process $L(\cdot)$. The property of infinite divisibility allows us to abstract away from the any grid discretization of space. Our key proposal here is to use stationary kernels defined as indicator functions $k(s, y) = 1_A(s - y)$ for some fixed indicator set A , such that the margins of the convolution process have distribution in the Lévy basis: $X(s) \sim F_A$. Therefore, tractable Lévy basis distributions F_A are preserved in the convolution process, which is not possible when using more general kernels on Lévy bases such as the gamma or inverse Gaussian ones, or on any other Lévy basis that is not stable. Moreover, modeling count data requires an integer-valued support; using discrete Lévy basis such as the Poisson or negative binomial ones in our indicator kernel approach allows generating integer-valued spatially dependent processes.

This flexible spatial modeling framework using indicator kernels may be viewed as an extension to *trawl processes*, which have been proposed for time series modeling [Barndorff-Nielsen et al. \(2014\)](#); [Noven et al. \(2015\)](#); [Grahovac et al. \(2017\)](#). To go beyond the very limited range of dependence structures in \mathbb{R}^d when smoothing a Lévy basis defined in \mathbb{R}^d with an indicator kernel, we will instead use a Lévy basis in \mathbb{R}^{d+1} with an indicator set defined as a *hypograph*, i.e., as the area between the hyperplane $s_{d+1} = 0$ and the surface $(s, H(s))$ with $s = (s_1, \dots, s_d)^T$ for a nonnegative function H called *height function*. Radially symmetric height functions H correspond to densities of a spherical probability distribution, which provides easily interpretable dependence models. If further H is non-increasing, we get nice and simple relationships in terms of the univariate distribution function of H between the set covariance function of the hypograph, the covariance function of $X(s)$ and the tail correlation function.

Section 2 presents generalities of the Lévy convolution approach. Modeling with hypographs is developed in Section 3; simulation techniques are shortly discussed in Section 3.3. Section 4 is dedicated to theoretical results on the tail behavior of the convolution process. Extensions to anisotropy and space-time modeling are treated in Section 5, which also puts forward several flexible latent process models. We develop parametric inference with a focus on pairwise likelihood in Section 6. The two applications of Section 7 demonstrate the versatility of our modeling framework, one to weed counts (Bjertop farm data), the other to Netherlands daily wind speed measurements. Concluding remarks and some perspectives are summarized in Section 8. Proofs are deferred to the Appendix.

2 Lévy convolution processes

2.1 Lévy bases

A Lévy basis L is a collection of random variables indexed by sets. We denote the Borel- σ -algebra in \mathbb{R}^d by $\mathcal{B}(\mathbb{R}^d)$, and $\mathcal{B}_b(\mathbb{R}^d)$ refers to its sets with finite Lebesgue measure. We just write \mathcal{B} and \mathcal{B}_b respectively when the reference to \mathbb{R}^d is clear. We call *random noise* any collection of \mathbb{R} -valued random variables $\{L(A) \mid A \in \mathcal{B}_b\}$ possessing the following property of additivity for any series of disjoint sets $A_j \in \mathcal{B}_b$, $j = 1, 2, \dots$, satisfying $\bigcup_{j=1}^{\infty} A_j \in \mathcal{B}_b$:

$$L\left(\bigcup_{j=1}^{\infty} A_j\right) = \sum_{j=1}^{\infty} L(A_j). \quad (1)$$

More specifically, a *Lévy basis* L on \mathbb{R}^d is a random noise satisfying two conditions: 1) independent scattering: $L(A_1) \perp L(A_2)$ if $A_1 \cap A_2 = \emptyset$ for $A_1, A_2 \in \mathcal{B}_b$; (2) infinite divisibility: for any $n \in \mathbb{N}$, we can represent L as the sum of n independent and identically distributed (iid) random measures $L_{n,1}, \dots, L_{n,n}$ such that $L \stackrel{d}{=} L_{n,1} + \dots + L_{n,n}$. The restriction to bounded sets \mathcal{B}_b avoids handling infinite volumes. Since bounded sets generate the full σ -algebra \mathcal{B} , no ambiguities or loss of generality arise. The probability distributions F_A of $L(A)$ in a Lévy basis are infinitely divisible; i.e., for any $n \in \mathbb{N}$, a distribution $F_{n,A}$ exists such that F_A is the n -fold convolution of $F_{n,A}$, written $F_A = F_{n,A}^{n*}$. The Lévy basis L is stationary if $L(s + A) = L(A)$ for any $s \in \mathbb{R}^d$ and $A \in \mathcal{B}_b$ with $s + A = \{s + y \mid y \in A\}$. In addition to being stationary, it is isotropic if $L(RA) = L(A)$ with $R \in \mathbb{R}^{d \times d}$ an orthogonal rotation matrix and $RA = \{Rs, s \in A\}$. Any setwise sum of Lévy bases is again a Lévy basis.

For statistical applications, we focus on Lévy bases for which $L(A)$ has tractable distribution F_A for sets of interest A . Well-known parametric form of F_A for any A is given by infinitely divisible distribution families that are closed under convolution of two iid random variables, such as the Gaussian, gamma, Cauchy, stable, Poisson or negative binomial families. The list of infinitely divisible parametric distributions with well-known expressions only for specific choices of A is much longer, containing distributions such as the student's t , Pareto, Gumbel, Fréchet, lognormal, inverse gamma and heavy-tailed Weibull ones. Other interesting constructions of infinitely divisible distributions do not possess a nice analytical form of the distribution function for any $A \neq \emptyset$; this is the case for most of the compound Poisson distributions defined through a sum of iid random variables with a Poisson-distributed number of terms. The characteristic function $\varphi(t; L(A)) = \exp(itL(A))$ of the variables $L(A)$ in a stationary Lévy basis L obeys the following Lévy-Khintchine formula:

$$\varphi(t; L(A)) = \exp\left(|A| \left[ita - bt^2/2 + \int_{\mathbb{R}} \{\exp(it y) - 1 - it y 1_{[-1,1]}(y)\} \eta(dy) \right] \right), \quad (2)$$

with $|A|$ the hypervolume of A , and deterministic parameters $a \in \mathbb{R}$, $b \geq 0$ and $\eta(\cdot)$ the so-called *Lévy measure* satisfying $\eta(\{0\}) = 0$ and $\int_{\mathbb{R}} \min(y^2, 1) \eta(dy) < \infty$. Conversely, any infinitely

divisible random variable L' has a representation as in (2), and we can use it as *Lévy seed* to define an isotropic stationary Lévy basis by fixing $L(A_1) \stackrel{d}{=} L'$ if $|A_1| = 1$; then Lévy variables $L(A)$ for any set A are determined by their characteristic function $\varphi(t; L')^{|A|}$. Given a stationary Lévy basis L , we will use the notation L' to designate a variable possessing same distribution as $L([0, 1]^d)$, and F' denotes the distribution of L' . In the following, we will assume that Lévy bases are isotropic and stationary if not explicitly stated otherwise.

In (2), the additive structure of $\log \varphi(t; L(A))$ reveals an additive decomposition of $L(A)$, and of the Lévy basis more generally, into three components. The value $a|A|$ is deterministic position parameter of F_A . If not explicitly stated otherwise, we assume $a \equiv 0$ in the following. The value of b characterizes the variance of an additive Gaussian component $W(A) \sim \mathcal{N}(0, b|A|)$ in $L(A) \stackrel{d}{=} W(A) + \tilde{L}(A)$. The complementary additive term $\tilde{L}(A)$ is independent of $W(A)$ and can be represented as the sum of the atom masses in A when considering a mixture of Poisson point processes with atoms of mass y ; we here refer to the latter component as the *pure jump part* of the Lévy basis.

Examples of Lévy bases are the Gaussian basis with $\eta \equiv 0$ (and $a = 0$ if it is centered), the Poisson basis with $b = 0$, $\eta(dx) = \lambda \delta_1(x) dx$ with intensity parameter $\lambda > 0$, or the gamma basis with $a = b = 0$ and $\eta(dx) = \alpha x^{-1} \exp(-\beta x) dx$ where $\alpha > 0$ is the shape and $\beta > 0$ the rate. We give more details on the gamma and inverse Gaussian Lévy bases, which will allow constructing nonnegative spatially dependent processes using our indicator kernel approach. The distributions in these Lévy bases are not stable since the convolution $F(\cdot) \star F(c(\cdot))$ is part of the basis only if $c = 1$, but not for general values $c > 0$. A stationary gamma Lévy basis satisfies $L(A) \sim \Gamma(\alpha|A|, \beta)$ with shape $\alpha|A|$ and rate $\beta > 0$; it has characteristic function

$$\varphi_\Gamma(t; L(A)) = \left(1 - \frac{it}{\beta}\right)^{-\alpha|A|}. \quad (3)$$

A stationary inverse gaussian Lévy basis satisfies $L(A) \sim \text{IG}(\lambda|A|^2, \mu|A|)$ with shape $\lambda|A|^2$ ($\lambda > 0$) and mean $\mu|A| > 0$ ($\mu > 0$); it has characteristic function (Chhikara and Folks, 1988)

$$\varphi_{\text{IG}}(t; L(A)) = \exp \left[|A| \mu \frac{\lambda}{\mu^2} \left(1 - \sqrt{1 - \frac{2\mu^2 it}{\lambda}} \right) \right]; \quad (4)$$

modifying A changes the mean to $\mu|A|$, while λ/μ^2 is invariant. For count data with overdispersion, the negative binomial (NB) distribution is an appropriate candidate, here parametrized as $\text{NB}(\mu, \theta)$ with the overdispersion parameter $\theta > 0$ and its mean μ ; its variance is $\mu + \mu^2/\theta$. The convolution of $\text{NB}(\mu_1, \theta_1)$ and $\text{NB}(\mu_2, \theta_2)$ with $\mu_1, \mu_2, \theta_1, \theta_2 > 0$ and $\mu_2/\mu_1 = \theta_2/\theta_1$ is $\text{NB}(\mu_1 + \mu_2, \theta_1 + \theta_2)$, *i.e.*, the convolution is additive in both parameters. A stationary NB Lévy basis satisfies $L(A) \sim \text{NB}(|A|\mu, |A|\theta)$ with characteristic function

$$\varphi_{\text{NB}}(t; L(A)) = \left(\frac{1-p}{1-p \exp(it)} \right)^{\theta|A|}, \quad p = \mu/(\mu + \theta). \quad (5)$$

2.2 Spatially dependent processes through kernel convolution

Process convolutions using a Lévy basis L on \mathbb{R}^d and an integrable kernel function $k : \mathbb{R}^d \times \mathbb{R}^d \rightarrow [0, \infty)$ have found widespread interest in the literature (e.g., [Higdon, 1998, 2002](#)) for modeling data through an isotropic stationary convolution process

$$X(s) = \int_{\mathbb{R}^d} k(s, y) L(dy), \quad (6)$$

which is well defined provided that mild integrability conditions are satisfied (e.g., [Barndorff-Nielsen et al., 2014](#)). If the variance $\sigma^2 > 0$ of L' is well-defined, the covariance function of $X(s)$ is

$$C(s) = \sigma^2 \int_{\mathbb{R}^d} k(y - s) k(s) dy. \quad (7)$$

If $k(\cdot)$ is not an *indicator kernel* (i.e., cannot be represented as an indicator function $c1_A(\cdot)$ with some set A and constant $c > 0$), the univariate distribution of $X(s)$ is in general not part of the Lévy basis, except for the case of a stable distribution F' . Tractability problems with likelihood-based approaches may arise; see [Wolpert and Ickstadt \(1998a\)](#); [Brix \(1999\)](#); [Kozubowski et al. \(2013\)](#), who sidestep this problem using simulation-based inference. Moreover, closed-form expressions of the covariance function $C(\cdot)$ are available only for specific choices of the kernel $k(\cdot)$. By contrast, indicator kernels yield marginal distributions of $X(s)$ that are still within the Lévy basis. For instance, the property of an exponential family such as the gamma or the inverse Gaussian Lévy bases allows using generalized additive modeling techniques for integrating covariate information into marginal distributions.

Non-Gaussian Lévy bases offer a wide panoply of moment properties, including skewness and heavy tails with undefined moments. Flexible univariate and multivariate marginal distributions may be created by adding process convolutions pertaining to different parametric families. For example, consider the sum of a Gaussian basis and a gamma basis, yielding so-called exponentially shifted Gaussian marginal distributions. The special case where the gamma convolution process is degenerated to an exponential random variable common to the whole space has been studied in [Krupskii et al. \(2017\)](#); [Krupskii and Genton \(2016\)](#).

2.3 Indicator convolution processes

We now consider the indicator convolution process $X(s) = L(s + A)$ defined over \mathbb{R}^d using a Lévy basis L on \mathbb{R}^d and the indicator set $A \in \mathcal{B}_b$. If $\text{Var}(L') = \sigma^2 < \infty$, the covariance function of $X(s)$ is $C(s) = \sigma^2 |A \cap (s + A)|$, which is the set covariance function of A rescaled by σ^2 . When second moments are not defined, we may still use the set covariance function for quantifying dependence in terms of the “size” of the additive random component $L(A \cap (s + A))$ that is common to two variables separated by the spatial lag s . To achieve spatial isotropy of $X(s)$, we further assume that A is a hyperball. If $d = 2$, then $A = A_\rho = \{s \in \mathbb{R}^2 \mid \|s\| \leq \rho\}$ is a disc of radius $\rho \geq 0$. We include points s with $\|s\| = \rho$ into A_ρ to get closed indicator sets. The resulting isotropic stationary

covariance function (with $u = \|s\|$) is

$$C(u; r) = \begin{cases} 2\rho^2 \left(\cos^{-1}(u/(2\rho)) - (u/2\rho) [1 - h^2/(2\rho^2)]^{1/2} \right), & 0 \leq u \leq 2\rho, \\ 0, & u > 2\rho. \end{cases} \quad (8)$$

One may use the approximation $C(u; \rho) \approx \pi\rho^2(1 - u/(2\rho))_+$ (Davison and Gholamrezaee, 2012). The covariance (8) has bounded support and decreases to 0 at approximately linear speed. To gain in flexibility, we could choose a random radius ρ , but such mixture modeling may be inappropriate in practice when only a single independent replication of the process $X(s)$ is observed, such that the mixture distribution cannot be identified. Flexible covariance functions with bounded or unbounded support may be obtained depending on the mixture distribution, but then closed-form expressions of $C(u)$ are generally not available. Instead, we propose to go beyond the restrictive dependence structure based on disc-shaped indicator sets in \mathbb{R}^2 by smoothing a Lévy basis in \mathbb{R}^3 , using so-called *hypograph kernels*.

3 Hypograph kernels

3.1 Hypographs

To generate isotropic stationary models, we define the indicator set A_H as the area enclosed between the surface $s_{d+1} = H(s_1, \dots, s_d)$ of a radially symmetric density function $H \geq 0$ (called *height function*) and the plane $s_{d+1} = 0$, corresponding to the (positive) *hypograph* of H denoted by $A_H = \{(s, h) \in \mathbb{R}^d \times [0, \infty) \mid 0 \leq H(s) \leq h\}$. To avoid identifiability issues between the distribution F' and the volume of the hypograph, we assume that $\int_{\mathbb{R}^d} H(s) ds = 1$ such that H is the probability density function of a d -variate spherical distribution. Moreover, by abuse of notation, we will throughout use the convention $s + A_H = \{(s, 0) + y \mid y \in A\}$ for $s \in \mathbb{R}^d$.

Flexible parametric models for $X(s)$ become available, and important differences arise in the dependence structure of $X(s)$ in contrast to the classical kernel convolution approach in (6) where the value of the kernel function is used to locally rescale a Lévy basis on \mathbb{R}^d before its aggregation over space. Intuition for spatial modeling suggests that what happens at a site s should be stronger influenced by what is happening close to the site than by what is happening farther away. Therefore, we will suppose that height functions are radially non-increasing such that $H(s_2) \leq H(s_1)$ if $\|s_2\| \geq \|s_1\|$, which will also simplify calculating covariance functions, see the following Section 3.2. Illustrations of hypograph convolution processes in \mathbb{R}^1 are given in Figure 1 for the Gaussian and gamma bases, and in Figure 2 for the Poisson basis; they are based on the Laplace density H resulting in an exponential correlation function; see Section 3.2. Figure 3 shows realizations of two spatial gamma convolution processes based on the bivariate spherical Gaussian density H resulting in a correlation function defined in terms of the univariate Gaussian survival function, see Section 3.2. The Lévy bases have been simulated using a discretization on a fine regular grid over $\mathbb{R} \times [0, H((0, 0)^T)]$; for a short exposition of alternative simulation techniques, see Section 3.3.

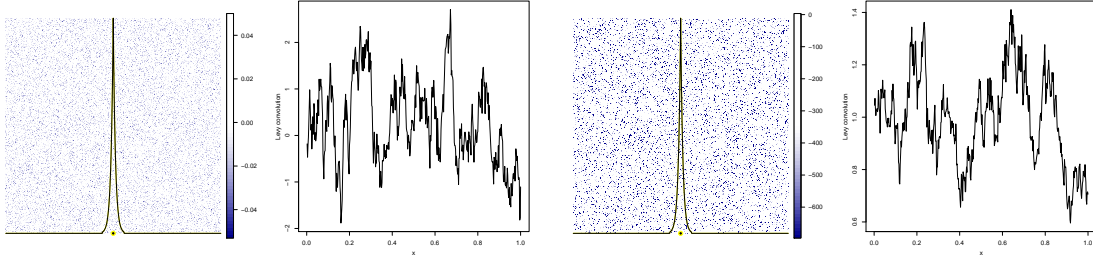


Figure 1: Hypograph convolution processes. Gaussian basis (1st display from the left) and gamma basis (3rd display, on log-scale) in \mathbb{R}^1 with height function given as the Laplace density. Gaussian convolution process (2nd display), gamma convolution process (4th display).

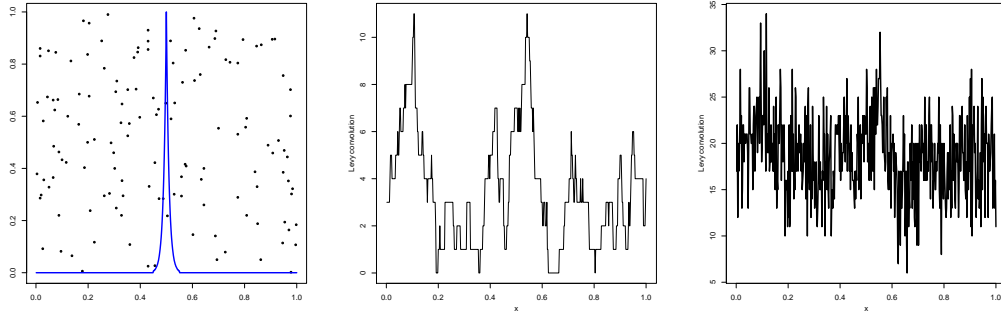


Figure 2: Hypograph convolution processes with Poisson basis (left) in \mathbb{R}^1 with height function given as the Laplace density. Middle: convolution process. Right: convolution process with additive Poisson nugget effect.

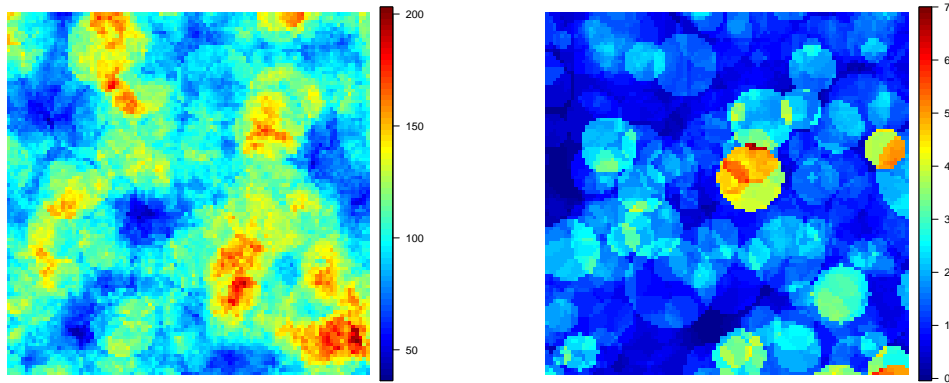


Figure 3: Hypograph convolution processes on $[0, 1]^2$ with gamma Lévy basis and height function given as the Gaussian density with standard deviation 0.05. Left: gamma convolution process with $\Gamma(20, 1/5)$ margins. Right: gamma convolution process with $\Gamma(2, 1)$ margins.

3.2 Hypograph covariance functions

We now suppose that L is an isotropic stationary Lévy basis with finite second moment $\sigma^2 = \text{Var}(L')$, and we consider the general case of a Lebesgue-integrable height function $H_s \geq 0$ that may depend on location s , such that the convolution process $X(s) = L(s + A_{H_s})$ may be nonstationary. The intersection of the hypographs centered at points s_1 and s_2 is $\{(s, h) \mid 0 \leq h \leq \min(H_{s_1}(s - s_1), H_{s_2}(s - s_2))\}$. We obtain the covariance function

$$C(s_1, s_2) = \sigma^2 \int \min(H_{s_1}(y - s_1), H_{s_2}(y - s_2)) dy, \quad s_1, s_2 \in \mathbb{R}^d. \quad (9)$$

Interestingly, when H_s are probability densities and $\sigma^2 = 1$, the class of correlation functions C in (9) coincides with the tail correlation functions of max-stable processes (Strokorob *et al.*, 2015, Section 2), which have been characterized in detail by Fiebig *et al.* (2017); Strokorob *et al.* (2015). In the stationary case with radially symmetric height function H , the covariance function is

$$C(s) = \sigma^2 \int \min(H(y - s), H(y)) dy, \quad s \in \mathbb{R}^d. \quad (10)$$

To obtain easily interpretable and flexible covariance functions C with closed-form expression of the integral in (10), we suppose that the height function H is radially non-increasing. Then, C can be expressed through the univariate survival function \bar{G} of the spherical distribution characterized by H . For points s that are closer to s_1 than to s_2 , we have $\min(H(s - s_1), H(s - s_2)) = H(s - s_2)$, and by symmetry we get $\min(H(s - s_1), H(s - s_2)) = H(s - s_1)$ when s is closer to s_2 . Writing $u = \|s_2 - s_1\|$, the part of the intersection that is closer to s_1 than to s_2 has hypervolume $1 - G(u/2) = \bar{G}(u/2)$, and by symmetry we get the same intersection volume for points closer to s_2 than to s_1 . Therefore, the correlation function is

$$C(u) = 2(1 - G(u/2)) = 2\bar{G}(u/2), \quad (11)$$

where $G(0) = 0.5$ owing to radial symmetry. Next, we present examples of interesting parametric models, ranging from a nugget effect and bounded dependence range to the exponential correlation function and long-tailed correlation functions.

Example 1 (Parametric correlation functions). *We use the notation $u = \|s\|$, and we fix $d = 2$ for simplicity.*

1. *Cylinder hypograph.* The cylinder-shaped height function with radius parameter $\rho > 0$, given as $H(s) = 1(u \leq \rho)/(\pi\rho^2)$, yields the correlation function presented in (8).
2. *Half-ball hypograph.* We set $H(s) = \sqrt{\rho^2 - (s_1^2 + s_2^2)}_+$, such that the hypograph corresponds to a half-ball of radius $\rho > 0$. Then,

$$C(u; \rho) = \pi(4\rho + u)(2\rho - u)^2/12 \text{ for } u < 2\rho, \quad C(u) = 0 \text{ for } h \geq 2\rho. \quad (12)$$

3. *Gaussian hypograph.* Setting $H(s) = (2\pi)^{-1}\rho^{-2} \exp(-u^2/(2\rho^2))$ with $\rho > 0$ yields $C(u; \rho) = 2\bar{\Phi}(u/(2\rho))$ where Φ is the univariate standard Gaussian distribution function.

4. *t* hypograph. Using the density of the spherical *t* distribution with dispersion parameter $\rho > 0$ and $\nu > 0$ degrees of freedom yields $C(u; \rho) = 2\bar{t}_\nu(u/(2\rho))$ where t_ν is the distribution function of the univariate standard *t* distribution.
5. Laplace hypograph. Using the spherical Laplace distribution with dispersion parameter $\rho > 0$ (Kotz et al., 2001), we get $\bar{G}(u) = 0.5 \exp(-u)$ and $C(u; \rho) = \exp(-u/\rho)$. The height function H has a singularity at the origin since $H(s) \rightarrow \infty$ when $u \rightarrow 0$.
6. Slash hypograph. Using the spherical slash distribution with scale parameter $\rho > 0$ (e.g., Wang and Genton, 2006) yields

$$\begin{aligned} C(u; \rho) &= 2(1 - [\Phi(u/(2\rho)) - \{\varphi(0) - \varphi(u/(2\rho))\}/(u/(2\rho))]) \\ &= 2\Phi(-u/(2\rho)) - 4(\sqrt{2\pi} - \varphi(u/(2\rho)))/(u/\rho), \quad u > 0, \end{aligned}$$

where the limit in 0 is $C(0) = 1$.

7. Nugget effect. The limit when $\rho \downarrow 0$ in the above examples can be interpreted as a nugget effect with the Dirac correlation function $C(u) = \delta_0(u)$.
8. Convex sums. A convex sum $\omega H_1 + (1 - \omega)H_2$, $\omega \in [0, 1]$, of two height functions leads to the correlation function $C(u) = \omega C_1(u) + (1 - \omega)C_2(u)$, with C_1 and C_2 the correlation functions associated to H_1 and H_2 respectively.

3.3 Simulation of hypograph convolution processes

Exact simulation of the Lévy basis L and hypograph convolution processes is well understood and straightforward for the Gaussian Lévy basis, where direct simulation of the Gaussian process $X(s)$ according to its covariance function can be done. The Poisson Lévy basis corresponds to a stationary spatial Poisson process, for which exact simulation is also feasible. For other models such as the gamma or the inverse Gaussian Lévy bases, the additive decomposition into the Gaussian and the pure jump part based on the characteristic function (see Section sec:levybasis) can be used for exact or approximate simulation with arbitrarily small approximation error; see Wolpert and Ickstadt (1998a) for this *Inverse Lévy measure* approach. An application to simulating spatial gamma Lévy basis has been implemented in Wolpert and Ickstadt (1998b).

In general, an approximate realization of $(X(s_1), \dots, X(s_m))^T$ for points s_j , $j = 1, \dots, m$, can be simulated by using a discretization of the Lévy basis on a fine grid spanning over a domain $D \times [0, h_{\max}]$ with $h_{\max} = \max_s H(s)$ (if it is finite) and D including the points s_j . A good approximation requires that the contribution of $L((s + A_H) \cap (D \times [0, h_{\max}])^C)$ to $X(s) = L(s + A_H)$ is negligible in practice. If densities and distribution functions are not available in closed form while the characteristic function is, the direct numerical inversion of the characteristic function makes it possible to calculate densities and distribution functions, which then allows simulation over space

discretized to a fine grid. Related tools are implemented in R packages such as **CharFun** (Simkova, 2017) or **prob** (Kerns, 2017).

Another approximation technique for smoothing a Lévy basis in \mathbb{R}^{d+1} according to a hypograph A_H may be to apply Cavalieri's principle (i.e., Fubini's theorem) to reduce the problem as follows: first, calculate a finite number m of independent Lévy convolution processes $X_i(s)$ in \mathbb{R}^d with disc-shaped kernels, then add them up to obtain an approximate simulation of $X(s)$. We now give some more details for $d = 2$. The simulation of a 3-dimensional Lévy basis L with Lévy seed L' and the calculation of $X(s_j) = L(s_j + A)$ are reduced to the computationally simpler problem of simulating m Lévy bases L_i in \mathbb{R}^2 and smoothing them with disc-shaped indicator kernels. The key idea is that smoothing a Lévy basis in \mathbb{R}^3 with a cylinder-shaped hypograph of radius ρ yields the same distribution of $X(s)$ as smoothing a Lévy basis in \mathbb{R}^2 with a disc-shaped indicator set of radius ρ . The Lévy basis in \mathbb{R}^2 is obtained by projecting the mass of the \mathbb{R}^3 basis for $s_3 \in [0, 1/(\rho^2\pi)]$ onto \mathbb{R}^2 . For an arbitrary continuous and radially non-increasing height function H , we approximate the radial function g in $H((r, w)) = g(r)/(2\pi)$ by a step function with $m \geq 1$ steps at radius values $r_0 = 0 < r_1 < \dots < r_m < r_{m+1} = \infty$, with steps of size $\rho_i = g(r_i) - g(r_{i+1})$, $i = 1, \dots, m$, and using the convention $g(r_{m+1}) = 0$. We approximate $X(s)$ through the sum of m hypograph convolution processes $X_i(s)$ with cylinder-shaped height functions of radius ρ_i , and the Lévy seed L'_i of L_i has characteristic function $\varphi(t; L'_i) = \varphi(t; L')^{1/(\rho_i^2/\pi)}$.

4 Extremal dependence behavior

A major benefit of non-Gaussian process convolutions is increased tail flexibility. We here show important results with respect to bivariate extremal dependence summaries. For any two functions a and b with $b(x) \neq 0$, we use the notation $a(x) \sim b(x)$ to indicate that $a(x)/b(x) \rightarrow 1$ when $x \rightarrow \infty$. We define the *tail correlation* χ of two random variables $X_1 \sim F_1$ and $X_2 \sim F_2$ as the conditional limit

$$\chi = \lim_{x \rightarrow \infty} \text{pr}(F_1(X_1) > 1 - 1/x \mid F_2(X_2) > 1 - 1/x) \in [0, 1] \quad (13)$$

if it exists, where $\chi > 0$ indicates asymptotic dependence while $\chi = 0$ corresponds to asymptotic independence (Coles *et al.*, 1999). In the case of asymptotic independence, joint tail decay rates are faster than marginal tail decay rates. Then, more precise information for a wide range of bivariate distributions can be obtained through the Ledford–Tawn representation (Ledford and Tawn, 1996)

$$\text{pr}(F_1(X_1) > 1 - 1/x, F_2(X_2) > 1 - 1/x) \sim \ell(x)x^{-1/\eta}, \quad x \rightarrow \infty, \quad (14)$$

with the *coefficient of tail dependence* $\eta \in (0, 1]$ and a slowly varying function $\ell(\cdot)$, i.e., $\ell(tx)/\ell(t) \rightarrow 1$ when $t \rightarrow \infty$. An alternative yet equivalent parametrization is through $\bar{\chi} = 2\eta - 1 \in (-1, 1]$ (Coles *et al.*, 1999), and we have

$$\bar{\chi} = \lim_{x \rightarrow \infty} \frac{\log \text{pr}(F_1(X_1) > 1 - 1/x)}{\log \text{pr}(F_1(X_1) > 1 - 1/x, F_2(X_2) > 1 - 1/x)}. \quad (15)$$

Incidentally, the value of $\bar{\chi}$ is the linear correlation coefficient in the case of a bivariate Gaussian distribution. In our set-up of isotropic stationary processes, we can define the summaries χ and $\bar{\chi}$ with respect to the distance between two sites s_1, s_2 .

We first collect some notations and definitions to provide useful results on tail dependence in stationary indicator convolution processes $X(s)$ based on a Lévy basis L . To simplify notations, we write $X_1 = L(A)$, $X_2 = L(s + A)$ with $X_1 \stackrel{d}{=} X_2$ the variables defined at sites $s_1 = 0$ and $s_2 = s$ based on their respective indicator sets A and $s + A$. Further, let $X_{12} = L(A \cap (s + A))$, $X_{1 \setminus 2} = L(A \setminus (s + A))$ and $X_{2 \setminus 1} = L((s + A) \setminus A)$. Clearly, these three variables X_{12} , $X_{1 \setminus 2}$, $X_{2 \setminus 1}$ are stochastically independent with

$$X_1 = X_{12} + X_{1 \setminus 2}, \quad X_2 = X_{12} + X_{2 \setminus 1}, \quad X_{1 \setminus 2} \stackrel{d}{=} X_{2 \setminus 1}, \quad (16)$$

such that X_{12} represents a “factor” that is common to X_1 and X_2 , while the residuals $X_{1 \setminus 2}$ and $X_{2 \setminus 1}$ of X_1 and X_2 respectively with respect to this factor are independent. For simplicity’s sake, we use the following notation for the hypervolumes of the indicator sets:

$$\alpha = |A|, \quad \alpha_0 = |A \cap (s + A)|, \quad \alpha_{\text{res}} = |A \setminus (s + A)|, \quad (17)$$

where $\alpha_{\text{res}} = |(s + A) \setminus A|$ by symmetry. We further write F_α for the distribution of a Lévy basis variable $L(A)$. Moreover, we denote by $\bar{F}(x) = 1 - F(x)$ the survival function of a distribution F , and by $F \star F$ the distribution of its convolution with itself. We now recall important tail distribution classes, which have been established in the literature and encompass many practically relevant infinitely divisible distributions. Depending on the class to which the Lévy basis pertains, we will show that structurally very different tail behavior arises in the convolution process.

Subexponential distributions are an important class of heavy-tailed distributions (Foss *et al.*, 2011). A distribution F is called subexponential if $\bar{F} \star \bar{F}(x)/\bar{F}(x) \sim 2$, where we additionally require that $F \star F$ is long-tailed when negative values arise with positive probability (Foss and Korshunov, 2007; Watanabe, 2008). Infinitely divisible subexponential distributions include the Weibull (with Weibull index smaller than 1), lognormal, Fréchet or Pareto ones and, more generally, all regularly varying distributions characterized by the limit relation

$$\bar{F}(tx)/\bar{F}(t) \rightarrow x^{-\gamma}, \quad t \rightarrow \infty, \quad x > 0, \quad (18)$$

with the regular variation index $\gamma > 0$. If $L(A)$ is subexponential for a set A , then all variables in the Lévy basis are subexponential, and we simply say that the Lévy basis is subexponential. In this case, we get $\bar{F}_{\alpha_1}(x)/\bar{F}_{\alpha_2}(x) \sim \alpha_1/\alpha_2$ for $\alpha_1, \alpha_2 > 0$, see Foss *et al.* (2011).

An important class of light-tailed distribution are those with exponential tails. We say that F has *exponential tail with rate* $\beta > 0$ if

$$\bar{F}(t+x)/\bar{F}(t) \rightarrow \exp(-\beta x), \quad t \rightarrow \infty, \quad (19)$$

for all x (e.g., Pakes, 2004; Watanabe, 2008). An exponential tail in $X \sim F$ is equivalent to a regularly varying distribution of $\exp(X)$ with index β . Two disjoint subclasses are the light-tailed

convolution-equivalent distributions satisfying $\mathbb{E} \exp(\beta X) < \infty$, and the gamma-tailed distributions satisfying $\mathbb{E} \exp(\beta X) = \infty$. We call F *convolution-equivalent with rate $\beta > 0$* if it is exponential-tailed with rate β and

$$\overline{F \star F}(x) / \overline{F}(x) \rightarrow 2m_F(\beta) < \infty, \quad m_F(\beta) = \int_{-\infty}^{\infty} \exp(\beta x) F(dx), \quad (20)$$

where $m_F(\beta)$ is the β -*exponentiated moment*. Any positive limit arising in (20) is necessarily $2m_F(\beta)$. All variables $L(A)$ in a Lévy basis with convolution-equivalent Lévy seed L' are convolution-equivalent with the same rate β (Theorem 3.1, Pakes, 2004), and we say that such a Lévy basis is convolution-equivalent. For instance, the inverse Gaussian distribution characterized in (4) is convolution-equivalent with $\beta = \lambda/(2\mu^2)$. In the exponential-tailed case where the β -exponentiated moment is not finite, we say that F is *gamma-tailed with rate β* if

$$\overline{F}(x) \sim \ell(x)x^{\alpha-1} \exp(-\beta x), \quad \alpha, \beta > 0, \quad (21)$$

with some slowly varying function ℓ . For instance, the variables $L(A)$ in a gamma Lévy basis are gamma-tailed with common rate parameter $\beta > 0$ and $\ell(x) = \Gamma(\alpha'\alpha)^{-1}$ if the Lévy seed satisfies $L' \sim \Gamma(\alpha', \beta)$, and we say that such a Lévy basis is gamma-tailed. Distributions with tail behavior (21), but where $\alpha < 0$ is negative, are convolution-equivalent (Lemma 2.3, Pakes, 2004). The following Proposition 1 treats the heavy-tailed set-up of subexponential Lévy bases, for which asymptotic dependence arises in the convolution process $X(s)$.

Proposition 1 (Asymptotic dependence in subexponential Lévy indicator convolutions). *Suppose that L is a subexponential Lévy basis. With notations as in (16) and (17), the tail dependence coefficient of the variables X_1 and X_2 for $A \neq \emptyset$ is*

$$\chi(X_1, X_2) = \frac{\alpha_0}{\alpha}. \quad (22)$$

The value of $\chi(X_1, X_2)$ can be interpreted as a variant of the set correlation function of A when A is shifted by the vector $(s, 0)$. Interestingly, the resulting tail correlation function $\chi(s)$ does not depend on the distribution of L except for the property of subexponentiality. Provided that L' has finite second moment, the linear correlation function and the tail correlation coincide for Lévy indicator convolutions, which transcribes the fact that co-movements in heavy-tailed variables are strongly determined by common additive components and tail events in particular. Next, we present a result for the gamma-tailed Lévy bases, which possess asymptotic independence in the convolution process $X(s)$.

Proposition 2 (Asymptotic independence in gamma-tailed Lévy indicator convolutions). *Suppose that L is a gamma-tailed Lévy basis where distributions F_α have rate parameter $\beta > 0$, shape parameter $\alpha > 0$ and slowly varying function ℓ_α as defined in (21). With notations as in (16) and (17), the variables X_1 and X_2 are asymptotically independent if $s \neq 0$, i.e. $\chi(s) = \delta_0(s)$, and we have $\bar{\chi}(X_1, X_2) = 1$. Moreover, if X_1 and X_2 are nonnegative, then*

$$\text{pr}(X_2 > x \mid X_1 > x) \sim \mathbb{E} \exp(\beta \min(X_{1 \setminus 2}, X_{2 \setminus 1})) \frac{\Gamma(\alpha)}{\beta \Gamma(\alpha_0) \Gamma(\alpha_{\text{res}}) \ell_{\text{res}}(x)} x^{-\alpha_{\text{res}}}. \quad (23)$$

Although gamma-tailed indicator convolution processes are asymptotically independent according to Proposition 2, the bivariate joint tail decay rate with $\eta(X_1, X_2) = 1$ is only moderately faster than the univariate tail decay rate.

Example 2 (Gamma Lévy basis). *For the gamma Lévy basis with $F_\alpha = \Gamma(\alpha, \beta)$, we have $\bar{\chi}(X_1, X_2) = 1$ and*

$$\text{pr}(X_2 > x \mid X_1 > x) \sim \mathbb{E} \exp(\beta \min(X_{1 \setminus 2}, X_{2 \setminus 1})) \frac{\Gamma(\alpha)}{\beta \Gamma(\alpha_0)} x^{-\alpha_{\text{res}}}.$$

Finally, we check the light-tailed convolution-equivalent indicator convolutions, for which asymptotic dependence arises in $X(s)$.

Proposition 3 (Asymptotic dependence in light-tailed convolution-equivalent Lévy indicator convolutions). *Suppose that L is a convolution-equivalent Lévy basis with rate parameter $\beta > 0$ as defined in (31). With notations as in (16) and (17), the variables X_1 and X_2 are asymptotically dependent if $\alpha_0 > 0$. Given the β -exponentiated moments $m_{L'}(\beta)$ of the Lévy seed L' and $\tilde{m}(\beta)$ of $\min(X_{1 \setminus 2}, X_{2 \setminus 1})$, we have*

$$\chi(X_1, X_2) = \frac{\alpha_0}{\alpha} \tilde{m}(\beta) m_{L'}(\beta)^{-\alpha_{\text{res}}}. \quad (24)$$

For an example, we consider the convolution-equivalent inverse Gaussian Lévy basis.

Example 3 (Inverse Gaussian Lévy basis). *The inverse Gaussian Lévy basis, for which $F_\alpha = \text{IG}(\lambda, \mu)$ with $L' \sim \text{IG}(\lambda, \mu_0)$, $\lambda, \mu_0 > 0$ and $\mu = \alpha \mu_0$, is known to be convolution-equivalent with rate $\lambda/(2\mu_0^2)$. Using Proposition 3 and $m_{L'}(\lambda/(2\mu_0^2)) = \exp(\lambda/\mu_0)$, we obtain*

$$\chi(X_1, X_2) = \frac{\alpha_0}{\alpha} \tilde{m}(\lambda/(2\mu_0^2)) \exp(-\alpha_{\text{res}} \lambda/\mu_0),$$

yielding asymptotic dependence if $\alpha_0 > 0$.

Interestingly, gamma-tailed Lévy bases yield asymptotic independence, while both the lighter-tailed convolution-equivalent bases and the heavier-tailed subexponential bases yield asymptotic dependence. Hence, a certain discontinuity arises in the tail dependence behavior when moving from lighter to heavier tails. Moreover, exponential-tailed Lévy bases can lead to both scenarios of asymptotic dependence or asymptotic independence in $X(s)$.

5 Modeling extensions

We discuss useful extensions beyond stationary and isotropic modeling. For obtaining nonstationary continuous marginal distributions, location-dependent shifting or rescaling of the convolution process $X(s)$ are straightforward approaches, and a combination with generalized additive modeling to capture covariate effects is possible. Nonstationary dependence can be achieved through location-dependent hypographs A_{H_s} , but calculations of intersecting hypervolumes may become

more intricate. A spatially independent component can be added to the convolution process to account for a nugget effect or observation errors.

Assuming isotropy is inappropriate when directional effects arise in spatial processes. We here adapt geometric anisotropy to the context of non-Gaussian Lévy convolutions by supposing that the isotropic convolution model applies after a rotation and rescaling of the coordinate system. Therefore, original coordinates \tilde{s} can be transformed to isotropic coordinates s using a rotation angle $\theta \in [0, \pi)$ and a stretching $b \geq 1$ along this direction,

$$s = \begin{pmatrix} b & 0 \\ 0 & 1 \end{pmatrix} \begin{pmatrix} \cos(\theta) & -\sin(\theta) \\ \sin(\theta) & \cos(\theta) \end{pmatrix} \tilde{s}. \quad (25)$$

Alternatively, one may conduct the geometric anisotropy transformation on indicator sets by defining the height function H as the density of an elliptically contoured probability distribution. However, calculating intersecting hypervolumes becomes more intricate and is related to the set covariance of ellipsoids.

The following two subsections focus on space-time modeling and on hierarchical modeling based on embedding a latent gamma indicator convolution respectively.

5.1 Space-time modeling

We propose two easily implementable possibilities to include temporal dependence into spatial models with data replicated in time, here with spatial dimension $d = 2$ for simplicity. The first model features a transport effect resulting from moving the hypograph through space according to a velocity vector $v = (v_1, v_2)^T$, such that $X(s, t) = L(s + vt + A_H)$. When the height function H is isotropic and radially decreasing and $\sigma^2 = \text{Var}(L')$, the covariance function is

$$C(s, t) = \sigma^2 \int_{\mathbb{R}^2} \min(H(0), H(s - vt)) \, ds = 2\sigma^2 \overline{G}(s - vt), \quad (26)$$

in analogy to (9). In general, C is nonseparable between space and time. Our second space-time separable model is for observations on a regular time grid, indexed without loss of generality by $t = 0, 1, 2, \dots$. For fixed t , we require that the spatial process $X(s, t)$ is a Lévy hypograph convolution with respect to a hypograph H . To define the temporal innovation structure, we use an additive decomposition of each spatial process for fixed t based on an iid series of spatial Lévy convolution processes. The time-dependent process $X(s, t)$ is constructed by adding components from $t, t - 1, \dots$ to generate the process at time t . For this purpose, we consider a discrete-time kernel $k_T(i)$, $i = 0, 1, \dots$, normalized such that $\sum_{i=0}^{\infty} k_T(i) = 1$; i.e., k_T is the probability mass function of a count distribution such as the Poisson, negative binomial or Zipf ones. Moreover, we assume monotonicity, $k_T(i + 1) \leq k_T(i)$, which makes sense when dependence strength decreases with time lag. If $i_{\max} < \infty$ exists such that $k_T(i_{\max}) > 0$ and $k_T(i) = 0$ for $i > i_{\max}$, the process $X(s, t)$ will be i_{\max} -dependent over time. We start with a sequence of iid Lévy bases L_t , $t \in \mathbb{Z}$. Next, we define Lévy hypograph convolutions $\{\varepsilon_{t,i}(s)\}$, $t \in \mathbb{Z}$, $i = 0, 1, \dots$, by applying the height

functions $k_T(i)H(\cdot)$ to each L_t , rescaled according to the time lag $i \geq 0$. The space-time convolution process is constructed as

$$X(s, t) = \sum_{i=0}^{\infty} \varepsilon_{t-i, i}(s). \quad (27)$$

The spatial covariance function C_S is associated to the hypograph A_H . Thanks to the monotonicity of k_T , we can calculate the separable space-time covariance function for $t_2 > t_1$,

$$\begin{aligned} C((s_1, t_1), (s_2, t_2)) &= \text{Cov} \left(\sum_{i=0}^{\infty} \varepsilon_{t_1, t_2-t_1+i}(s_1), \sum_{i=0}^{\infty} \varepsilon_{t_1, t_2-t_1+i}(s_2) \right) \\ &= \sum_{i=0}^{\infty} \text{Cov} (\varepsilon_{t_1, t_2-t_1+i}(s_1), \varepsilon_{t_1, t_2-t_1+i}(s_2)) \\ &= C_S(s_1, s_2) \sum_{i=0}^{\infty} k_T(t_2 - t_1 + i) \\ &= C_S(s_1, s_2) C_T(t_2 - t_1), \end{aligned}$$

whose temporal correlation function $C_T(t_2 - t_1) = \sum_{i=0}^{\infty} k_T(t_2 - t_1 + i)$ is the survival function of the distribution k_T .

5.2 Latent Gamma process models

For hierarchical modeling, we may embed a Lévy convolution process for a parameter related to the central tendency of the univariate data distribution. Specifically, a latent gamma indicator convolution process $G(s)$ provides useful hierarchical models. Embedding $G(s)$ for the rate of an exponential distribution yields generalized Pareto margins. [Bacro *et al.* \(2017\)](#) have used this to construct space-time models for asymptotically independent threshold exceedances by using indicator sets defined as slated cylinders in space-time, and closed-form expressions of bivariate distributions arise. In their construction, the space-time gamma indicator convolution $G(s, t)$ drives both the exceedances and the exceedance probability $p(s, t) = \exp(-X(s, t))$. Embedding $G(s)$ for the mean of a Poisson distribution yields negative binomial (NB) margins ([Hilbe, 2011](#)). The NB parameter θ in (5) corresponds to the gamma shape parameter. Using bivariate results for negative binomial distributions derived in [Cameron and Trivedi \(2013, Section 8.4.2\)](#), closed-form representations of bivariate probability mass functions of the hierarchical process can be obtained.

A spatial inverted max-stable process ([Wadsworth and Tawn, 2012](#)) is obtained when embedding an indicator convolution process with positive α -stable Lévy basis ($0 < \alpha < 1$) for the rate of an exponential distribution. Indeed, multivariate distributions have logistic max-stable dependence ([Stephenson, 2009](#)), and the resulting convolution process has structure very similar to the inverted Reich–Shaby model ([Reich and Shaby, 2012](#)).

6 Pair-based inference

Our modeling framework provides a natural link between marginal distributions and dependence structure, which avoids a full separation of margins and dependence such as in copula modeling. We therefore suppose that the data process can directly be modeled by a Lévy indicator convolution process, or after applying an easily tractable and interpretable marginal transformation, or by a latent Lévy process model. Knowing the parametric family of marginal distributions allows us to separate the estimation of Lévy basis parameters from those related to the shape of the kernel, and approaches such as the independence likelihood (Varin *et al.*, 2011) can be used to estimate the Lévy basis parameters and to select an appropriate model. If the covariance function of the Lévy indicator convolution process $X(s)$ is well defined, standard geostatistical techniques are available to estimate parameters by contrasting empirical and model covariance functions (Chiles and Delfiner, 2009). This method may also be used to provide good starting values for iteratively maximizing pairwise likelihood functions, which will be the focus of the remainder of this section.

Pairwise likelihood approaches are composite likelihood techniques, whose estimation efficiency and asymptotic properties are close to classical maximum likelihood estimation under mild conditions (Varin *et al.*, 2011). Bivariate vectors in Lévy indicator convolutions can be expressed through three independent components X_{12} , $X_{1\setminus 2}$ and $X_{2\setminus 1}$ defined in (16) and (17). If densities of these base variables are fast to compute, pairwise densities can be computed by integrating out one of the components, here chosen as X_{12} . If θ denotes the parameter vector to be estimated, the likelihood contribution of a pair (x_1, x_2) observed at s_1 and s_2 amounts to

$$\ell(\theta; x_1, x_2) = \begin{cases} \int_{\mathbb{R}} f_{X_{1\setminus 2}}(x_1 - y) f_{X_{2\setminus 1}}(x_2 - y) f_{X_{12}}(y) dy, & \alpha_0 \neq 0, \\ f_{X_1}(x_1) f_{X_2}(x_2), & \alpha_0 = 0. \end{cases} \quad (28)$$

In the case of a nonnegative integer-valued Lévy basis for modeling count data, the integral is replaced by a finite sum and $\ell(x_1, x_2)$ can always be calculated exactly:

$$\ell(\theta; x_1, x_2) = \sum_{y=0}^{\min(x_1, x_2)} f_{X_{1\setminus 2}}(x_1 - y) f_{X_{2\setminus 1}}(x_2 - y) f_{X_{12}}(y). \quad (29)$$

With continuous Lévy basis distributions, we can always calculate the pairwise likelihood (28) through numerical integration, while closed-form expressions are available in some cases. In some cases, variants of pairwise likelihood allow us to bypass the calculation of the numerical integrals in (28), which may be rather costly when data sets are large. The difference likelihood for the difference of variables $X(s_2) - X(s_1) = X_{1\setminus 2} - X_{2\setminus 1}$ is related to the difference of two independent variables and may be better tractable. For instance, with gamma Lévy indicator convolutions it corresponds to the difference of two iid gamma variables, a special case of the variance-gamma distribution (Madan and Seneta, 1990). A closed-form density can be written in terms of the modified Bessel function of the second kind K_ν . If $L' \sim \Gamma(\alpha', \beta)$, $\tilde{\alpha} = \alpha' \alpha_1$ and $x = x_2 - x_1$, we get

$$\ell_{\Gamma, \text{diff}}(\theta; x) = \frac{\beta^{2\tilde{\alpha}} |x|^{\tilde{\alpha}-1/2} K_{\tilde{\alpha}-1/2}(\beta|x|)}{\sqrt{\pi} \Gamma(\tilde{\alpha}) (2\beta)^{\tilde{\alpha}-1/2}}, \quad x \in \mathbb{R}. \quad (30)$$

In general, estimation performance of such pairwise difference likelihoods remains comparable to the more classical pairwise marginal likelihood, see the study of [Bevilacqua and Gaetan \(2015\)](#) in the context of Gaussian processes.

7 Application examples

7.1 Bjertorp farm weed counts

Figure 4 illustrates the data consisting of weed counts for 100 areal units of an agricultural field at the Bjertorp farm in Sweden ([Guillot *et al.*, 2009](#)). Due to spatial dependence, we have no structure of independent replication for this data. The count sample has a mean of 81 with an empirical standard deviation of 61, hinting at strong overdispersion. For isotropic stationary modeling, we consider Lévy hypograph convolutions of Poisson or negative binomial (NB) type, and we further allow for a nugget of Poisson or NB type respectively. Estimation is done by numerical maximization of the pairwise likelihood (PL) in (29) using all pairs. For the height function H , we use the bivariate spherical probability densities of cylinder-shaped, Gaussian, Laplace or Cauchy type; the latter is a student's t density with degree of freedom $\nu = 1$ and has power-law tail implying long-range dependence. Our hypograph models have only one parameter for the range to account for the small sample size with only one temporal replicate. For model selection, we focus on maximum PL values since, owing to strong spatial dependence, calculating formal criteria such as the composite likelihood information criterion (CLIC, [Varin and Vidoni, 2005](#)) would be intricate even when based on block bootstrap techniques.

Models with Poisson Lévy basis have much lower PL values (unreported) with relatively small variation between different models as compared to the NB basis; we attribute this to the strong overdispersion observed empirically, and we therefore do not report estimates for Poisson models. Table 1 summarizes estimated hypograph parameters characterizing dependence and reports PL values for NB models. For each hypograph model, fitted with or without nugget, we have considered two estimation techniques: either with all parameters estimated in a single step, or with the negative binomial mean μ fixed to the empirical mean of observations when estimating the remaining parameters through PL. Table 1 reports only the results for the single step estimation since differences in log-likelihood values and estimated values between the two estimation procedures turned out to be small. A plausible explanation is that the mean parameter is very well identifiable even in our setting with relatively few data, which is also confirmed by small differences in estimated means over all models.

Optimal log-PL values are very similar except for the Cauchy model, whose values are by approximately 20 lower than the others. The best model turns out to be the cylinder-shaped hypograph with nugget, whose relative additive contribution to the mean is estimated to be 0.21. With Cauchy and Laplace models, finding good starting values for identifying a nugget value that improves upon the model without nugget was not possible, and we report an estimate of approx-

Hypograph	log-PL	mean $\hat{\mu}$	scale $\hat{\rho}$	overdisp. $\hat{\theta}$	rel. nugget
cylinder	-53020	82.8	36.3	0.0185	—
	-53016	82.7	42.2	0.0185	0.21
Gaussian	-53019	82.7	22.5	0.0185	—
	-53018	82.7	24.3	0.0185	0.1
Laplace	-53038	82.8	6.14	0.0185	—
	-53038	82.8	6.14	0.0185	0
Cauchy	-53021	82.7	33.9	0.0185	—
	-53021	82.7	33.9	0.0185	0

Table 1: Maximum pairwise log-likelihood and estimates for the negative binomial Lévy hypograph convolution models fitted to the Bjertop weed count data.

imately 0. The count proportion of 0.21 explained by the nugget reduces the spatial dependence in comparison to the same model with nugget set to 0; this effect is reflected in our estimates by a larger dependence range 42.2 with nugget while it is 36.3 without. Model fits suggest that hypographs with relatively low values at larger distances perform slightly better in comparison to the Laplace (exponential decay) and Cauchy (power decay) ones, suggesting that dependence is relatively strong at small distances but then decays strongly. An interpretation is that the seeds at the origin of the observed weeds were dispersed groupwise (e.g., through moving air masses) with a typical within-group scattering range. Alternative, seeds from existing weeds in this agricultural field may have been dispersed within a relatively small and well defined range, leading to spatial clusters of weeds and grouping patterns. We refer to [Soubeyrand *et al.* \(2011\)](#) for more details on kernel-based modeling theory for group patterns, which can be characterized by stochastic models with spatial dependence.

7.2 Daily wind speeds in the Netherlands

We here propose spatial dependence modeling for daily maximum wind gust data, collected between November 14, 1999 and November 13, 2008 at 30 measurement sites spread over the Netherlands (see www.knmi.nl for public access to those data). Extreme value studies of wind speed data ([Ledford and Tawn, 1996](#); [Opitz, 2016](#); [Huser *et al.*, 2017](#)) show strong support for asymptotic independence. For the present data, [Opitz \(2016\)](#) provided arguments in favor of an asymptotically independent Gaussian scale mixture model with slower joint tail decay than for Gaussian processes. In general, the Weibull distribution provides a satisfactory fit for the univariate distributions of wind speed data (e.g., [Stevens and Smulders, 1979](#); [Seguro and Lambert, 2000](#); [Akdağ and Dinler, 2009](#)), such that we here propose to power-transform a spatial gamma Lévy convolution process with exponential margins to model the data and their spatial dependence. As shown in [Example 2](#), gamma convolutions have relatively strong dependence in asymptotic dependence with coefficient $\bar{\chi} = 1$, and can therefore be considered as suitable models in the light of the empirical findings of the aforementioned studies. Similar to [Opitz \(2016\)](#), we use the independence likelihood to

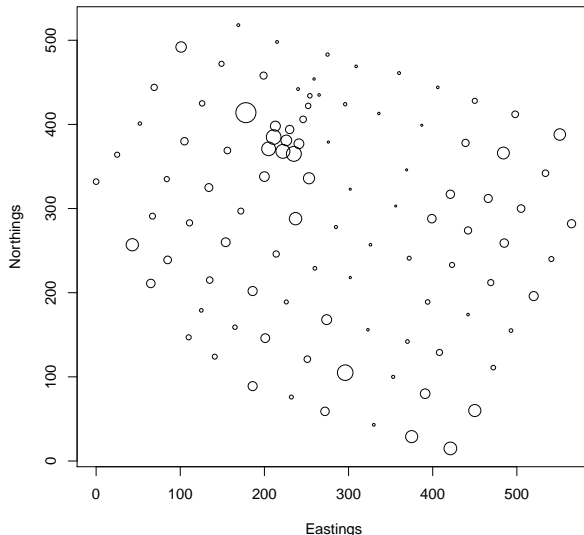


Figure 4: Spatial weed count data from the Bjertop farm (Sweden). Disc surfaces are proportional to counts.

fit the marginal Weibull model with estimated Weibull index 2.63 and the log-scale estimated as $2.69 - 0.0017 \times \text{dist}$, where dist is the distance to the North Sea coast. Then, data are station-wise pretransformed to a standard exponential marginal scale using the fitted Weibull distribution.

We fix $L' \sim \Gamma(1, 1)$, such that marginal distributions in the fitted hypograph convolution processes are standard exponential. We fit hypographs of cylinder-shaped, Gaussian, Laplace, Cauchy or student's t type for the dependence, and we test both isotropic or geometrically anisotropic models according to the space transformation presented in (25). The pairwise difference likelihood in (30) is used, and estimation results are reported in Table 2. According to the composite likelihood information criterion (CLIC, Varin and Vidoni, 2005), here estimated through a block bootstrap approach (Carlstein, 1986), the Cauchy hypograph model comes out best, suggesting long-range dependence in wind speeds. We point out that CLIC gains due to anisotropy tend to be more important than differences between hypographs for anisotropic models, which is in line with results of Opitz (2016) obtained for threshold exceedance data.

8 Discussion

We have developed a flexible and tractable modeling framework based on Lévy bases smoothed by indicator kernels, which allows working with distribution properties related to tail structure and dependence that go far beyond the ubiquitous Gaussian processes. The practical potential of such processes to bridge asymptotic dependence classes in a natural way through the choice of the Lévy basis family should be further studied; we refer to Wadsworth *et al.* (2017) for some

Hypograph	scale	nugget	aniso:angle $\hat{\theta}$	aniso:scale \hat{b}	CLIC
cylinder	648(42)	0.286(0.0056)	—(—)	—(—)	717700
	754(41)	0.284(0.0054)	1.24(0.06)	1.46(0.052)	717335
Gaussian	513(31)	0.286(0.0063)	—(—)	—(—)	717702
	596(38)	0.283(0.0052)	1.24(0.058)	1.46(0.049)	717435
Laplace	1160(72)	0.283(0.0047)	—(—)	—(—)	717539
	1360(89)	0.281(0.0058)	1.25(0.062)	1.47(0.058)	717493
Cauchy	402(27)	0.285(0.0056)	—(—)	—(—)	717707
	467(28)	0.283(0.0049)	1.25(0.064)	1.47(0.056)	717320
student's t	339(29)	0.284(0.0086)	—(—)	—(—)	717691
	467(28)	0.283(0.0052)	1.25(0.057)	1.46(0.053)	717345

Table 2: Estimation results for gamma Lévy hypograph convolution models fitted to the Netherlands wind speed data. Standard errors based on a block bootstrap are given in parentheses. The last columns reports the CLIC with lower values indicating better fit. The estimate $1/\nu$ for the inverse degree of freedom parameter of student's t model is 1.83(4.58) for the isotropic model and 0.985(0.334) for the anisotropic model, implying a heavier-tailed covariance function when neglecting anisotropy in data.

background on models covering both asymptotic dependence and independence. Moreover, sums of two convolution processes, one with bounded dependence range and asymptotic dependence, the other with asymptotic independence, would yield random field models where the asymptotic dependence range is bounded.

Spatial modeling of count data becomes feasible using pairwise likelihood, where latent process constructions are optional but not necessary. With Lévy bases suitable for count data such as the Poisson one, our approach generalizes the multivariate models of [Karlis and Meligkotsidou \(2005\)](#) and the time series models of [Barndorff-Nielsen *et al.* \(2014\)](#) to the spatial or space-time set-up. A physical interpretation of indicator kernels is straightforward when observed count values have been aggregated over overlapping areas of the study region. [Wakefield \(2006\)](#) states that “there are currently no simple ways of fitting frequentist fixed-effects, nonlinear models with spatially dependent residuals”. An extension of count modeling based on Lévy indicator convolutions, used either directly or as a Poisson mean in hierarchical approaches, towards including covariates in a flexible nonstationary model appears to be a promising solution to this problem and is part of prospected work.

More generally, using Lévy indicator convolutions to obtain spatially dependent residuals in regression modeling paves the way towards tractable frequentist inference based on composite likelihood. Nonstationary spatial convolution processes such as those envisaged for regression modeling can be generated by using nonstationary kernels, a nonstationary Lévy basis or deterministic rescaling or shifting of a first-order stationary convolution process, and several of such techniques may be combined. Future work could explore the model properties and efficient inference for such models.

Efforts should also go into fast and accurate simulation techniques, in particular for conditional simulation, which is more intricate than for the Gaussian case. This could further pave the way

for simulation-based Bayesian inference of parameters, which would be an important alternative in cases where estimation uncertainty is high, such as in our application to spatial weed counts without temporal replication.

Appendix

Proof of Proposition 1. Using the definition of χ , we get

$$\chi(X_1, X_2) = \lim_{x \rightarrow \infty} \frac{\overline{F_{\alpha_0} \star F_{\min(X_1, X_2)}}(x)}{\overline{F_{\alpha}}(x)}, \quad x \rightarrow \infty,$$

where $\overline{F_{\min(X_1, X_2)}}(x) \sim \overline{F_{\alpha_{\text{res}}}}^2(x)$. The tail property $\overline{F_{\alpha_1}}(x)/\overline{F_{\alpha_2}}(x) \sim \alpha_1/\alpha_2$ of subexponential distributions gives $\overline{F_{\min(X_1, X_2)}}(x)/\overline{F_{\alpha_0}}(x) \rightarrow 0$, and applying Foss and Korshunov (Theorem 9, 2007) then yields $\overline{F_{\alpha_0} \star F_{\min(X_1, X_2)}}(x) \sim \overline{F_{\alpha_0}}(x)$. Using this, we prove the assertion $\chi(X_1, X_2) = \alpha_0/\alpha$. \square

To prove the joint tail decay results in the gamma-tailed case, we first recall a result on gamma-tailed convolutions in the following Lemma 4.

Lemma 4 (Convolution of exponential-type random variable, see Theorem 1.1 of Hashorva and Li (2014)). *For two nonnegative gamma-tailed distributions F_1, F_2 satisfying*

$$\overline{F_i}(x) \sim \ell_i(x)x^{\alpha_i-1} \exp(-\beta x), \quad \beta > 0, \alpha_i > 0, \quad i = 1, 2, \quad (31)$$

with slowly varying functions ℓ_i , we get

$$\overline{F_1 \star F_2}(x) \sim \beta \frac{\Gamma(\alpha_1)\Gamma(\alpha_2)}{\Gamma(\alpha_1+\alpha_2)} \ell_1(x)\ell_2(x)x^{\alpha_1+\alpha_2-1} \exp(-\beta x), \quad x \rightarrow \infty. \quad (32)$$

Proof of Proposition 2. Since $\text{pr}(\min(X_{1\setminus 2}, X_{2\setminus 1}) > x) \sim \text{pr}(X_{1\setminus 2} > x)^2$, the minimum of $X_{1\setminus 2}$ and $X_{2\setminus 1}$ is exponential-tailed with rate $2\beta > \beta$. Applying Breiman's lemma to $\exp(\min(X_1, X_2))$, see Pakes (2004, Lemma 2.1), we obtain

$$\text{pr}(\min(X_1, X_2) > x) \sim \mathbb{E} \exp(\beta \min(X_{1\setminus 2}, X_{2\setminus 1})) \text{pr}(X_{12} > x). \quad (33)$$

We calculate the limit $\bar{\chi}(X_1, X_2)$ in (15) using (33) and (31), which yields $\bar{\chi} = \eta = 1$. Next, Lemma 4 confirms that $\alpha = \alpha_0 + \alpha_{\text{res}}$, and it proves

$$\begin{aligned} \text{pr}(X_1 > x) &= \text{pr}(X_{12} + X_{1\setminus 2} > x) \sim \beta \frac{\Gamma(\alpha_0)\Gamma(\alpha_{\text{res}})}{\Gamma(\alpha)} \ell_0(x)\ell_{\text{res}}(x)x^{\alpha-1} \exp(-\beta x) \\ &= \beta \frac{\Gamma(\alpha_0)\Gamma(\alpha_{\text{res}})}{\Gamma(\alpha)} \ell_{\text{res}}(x)x^{\alpha_{\text{res}}-1} \text{pr}(X_{12} > x), \end{aligned} \quad (34)$$

with ℓ_0 the slowly varying function in (21) of X_{12} . By injecting formulas (34) and (33) into the conditional probability

$$\text{pr}(X_2 > x \mid X_1 > x) = \frac{\text{pr}(\min(X_1, X_2) > x)}{\text{pr}(X_1 > x)}, \quad (35)$$

Equation (23) follows, and clearly $\chi(X_1, X_2) = 0$ if $\alpha_{\text{res}} > 0$, that is, if $s \neq 0$. \square

Proof of Proposition 3. Pakes (2004, Theorem 3.1) shows that the survival function of a convolution-equivalent infinitely divisible distribution F_α is tail-equivalent to its Lévy measure $\alpha\eta(\cdot)$ (as defined by (2)) in the following sense:

$$\overline{F}_\alpha(x) \sim m_{F_\alpha}(\beta) \alpha\eta[x, \infty), \quad (36)$$

where $m_{F_\alpha}(\beta) = m_{L'}(\beta)^\alpha$ owing to infinite divisibility. In analogy to the proof of Proposition 2 for gamma-tailed Lévy bases, the minimum of $X_{1\setminus 2}$ and $X_{2\setminus 1}$ is exponential-tailed with rate $2\beta > \beta$, and applying Breiman's lemma to $\exp(\min(X_1, X_2))$ gives

$$\text{pr}(\min(X_1, X_2) > x) \sim \tilde{m}(\beta) \text{pr}(X_{12} > x). \quad (37)$$

By writing the tail representation (36) of X_{12} with α replaced by α_{res} and combining (36) and (37), the value of $\chi(X_1, X_2)$ can be calculated,

$$\chi(X_1, X_2) = \lim_{x \rightarrow \infty} \frac{\tilde{m}(\beta)^{\alpha_0} m_{F_{\alpha_0}}(\beta) \eta[x, \infty)}{\alpha m_{F_\alpha}(\beta) \eta[x, \infty)} = \frac{\alpha_0}{\alpha} \tilde{m}(\beta) m_{L'}(\beta)^{-\alpha_{\text{res}}},$$

where we have used $m_{F_{\alpha_0}}(\beta) = m_{L'}(\beta)^{\alpha_0}$. □

References

- Akdağ, S. A. and Dinler, A. (2009) A new method to estimate Weibull parameters for wind energy applications. *Energy conversion and management* **50**(7), 1761–1766.
- Bacro, J.-N., Gaetan, C., Opitz, T. and Toulemonde, G. (2017) Hierarchical space-time modeling of exceedances with an application to rainfall data. *arXiv:1708.02447*.
- Banerjee, S., Carlin, B. P. and Gelfand, A. E. (2014) *Hierarchical modeling and analysis for spatial data*. CRC Press.
- Barndorff-Nielsen, O. E., Lunde, A., Shephard, N. and Veraart, A. E. D. (2014) Integer-valued trawl processes: A class of stationary infinitely divisible processes. *Scandinavian Journal of Statistics* **41**(3), 693–724.
- Barndorff-Nielsen, O. E., Mikosch, T. and Resnick, S. I. (2012) *Lévy processes: theory and applications*. Springer.
- Bevilacqua, M. and Gaetan, C. (2015) Comparing composite likelihood methods based on pairs for spatial Gaussian random fields. *Statistics and Computing* **25**(5), 877–892.
- Bousset, L., Jumel, S., Garreta, V., Picault, H. and Soubeyrand, S. (2015) Transmission of leptosphaeria maculans from a cropping season to the following one. *Annals of Applied Biology* **166**(3), 530–543.
- Brix, A. (1999) Generalized gamma measures and shot-noise Cox processes. *Advances in Applied Probability* **31**(4), 1929–1953.
- Calder, C. A. (2008) A dynamic process convolution approach to modeling ambient particulate matter concentrations. *Environmetrics* **19**(1), 39–48.

- Cameron, A. C. and Trivedi, P. K. (2013) *Regression analysis of count data*. Cambridge University Press.
- Carlstein, E. (1986) The use of subseries values for estimating the variance of a general statistic from a stationary sequence. *The Annals of Statistics* **14**(3), 1171–1179.
- Chhikara, R. and Folks, J. L. (1988) *The Inverse Gaussian Distribution: Theory, Methodology, and Applications*. CRC Press.
- Chiles, J.-P. and Delfiner, P. (2009) *Geostatistics: modeling spatial uncertainty*. John Wiley & Sons.
- Coles, S., Heffernan, J. and Tawn, J. (1999) Dependence measures for extreme value analyses. *Extremes* **2**(4), 339–365.
- Davison, A. C. and Gholamrezaee, M. M. (2012) Geostatistics of extremes. *Proceedings of the Royal Statistical Society (Series A)* **468**(2138), 581–608.
- Fiebig, U.-R., Strokorb, K. and Schlather, M. (2017) The realization problem for tail correlation functions. *Extremes* **20**(1), 121–168.
- Foss, S. and Korshunov, D. (2007) Lower limits and equivalences for convolution tails. *The Annals of Probability* **35**(1), 366–383.
- Foss, S., Korshunov, D. and Zachary, S. (2011) *An introduction to heavy-tailed and subexponential distributions*. Springer.
- Grahovac, D., Leonenko, N. N. and Taqqu, M. S. (2017) Intermittency of trawl processes. *arXiv preprint arXiv:1708.02762*.
- Guillot, G., Lorén, N. and Rudemo, M. (2009) Spatial prediction of weed intensities from exact count data and image-based estimates. *Journal of the Royal Statistical Society: Series C (Applied Statistics)* **58**(4), 525–542.
- Hashorva, E. and Li, J. (2014) Asymptotics for a discrete-time risk model with the emphasis on financial risk. *Probability in the Engineering and Informational Sciences* **28**(4), 573–588.
- Hellmund, G., Prokesova, M. and Jensen, E. B. V. (2008) Lévy-based Cox point processes. *Advances in Applied Probability* pp. 603–629.
- Higdon, D. (1998) A process-convolution approach to modelling temperatures in the North Atlantic Ocean. *Environmental and Ecological Statistics* **5**(2), 173–190.
- Higdon, D. (2002) Space and space-time modeling using process convolutions. In *Quantitative methods for current environmental issues*, ed. C. P. E.-S. A. Anderson C.W., Barnett V., pp. 37–56. Springer.
- Hilbe, J. M. (2011) *Negative binomial regression*. Cambridge University Press.
- Huser, R., Opitz, T. and Thibaud, E. (2017) Bridging asymptotic independence and dependence in spatial extremes using Gaussian scale mixtures. *Spatial Statistics* **21**, 166–186.
- Joe, H. (2014) *Dependence modeling with copulas*. CRC Press.
- Jónsdóttir, K. Ý., Rønn-Nielsen, A., Mouridsen, K. and Vedel Jensen, E. B. (2013) Lévy-based

- modelling in brain imaging. *Scandinavian Journal of Statistics* **40**(3), 511–529.
- Karlis, D. and Meligkotsidou, L. (2005) Multivariate poisson regression with covariance structure. *Statistics and Computing* **15**(4), 255–265.
- Kerns, G. J. (2017) *prob: Elementary Probability on Finite Sample Spaces*. R package version 1.0-0.
- Kotz, S., Kozubowski, T. J. and Podgorski, K. (2001) *The Laplace distribution and generalizations: a revisit with applications to communications, economics, engineering, and finance*. Birkhäuser.
- Kozubowski, T. J., Podgorski, K. and Rychlik, I. (2013) Multivariate generalized Laplace distribution and related random fields. *Journal of Multivariate Analysis* **113**, 59–72.
- Krupskii, P. and Genton, M. G. (2016) A copula-based linear model of coregionalization for non-gaussian multivariate spatial data. *arXiv preprint arXiv:1603.03950* .
- Krupskii, P., Huser, R. and Genton, M. G. (2017) Factor copula models for replicated spatial data. *Journal of the American Statistical Association* (In press).
- Ledford, A. W. and Tawn, J. A. (1996) Statistics for near independence in multivariate extreme values. *Biometrika* **83**(1), 169–187.
- Madan, D. B. and Seneta, E. (1990) The variance gamma (VG) model for share market returns. *Journal of business* **63**(4), 511–524.
- Mikosch, T. (2006) Copulas: Tales and facts. *Extremes* **9**(1), 3–20.
- Noven, R. C., Veraart, A. E. D. and Gandy, A. (2015) A latent trawl process model for extreme values. *arXiv preprint arXiv:1511.08190* .
- Opitz, T. (2016) Modeling asymptotically independent spatial extremes based on Laplace random fields. *Spatial Statistics* **16**, 1–18.
- Pakes, A. G. (2004) Convolution equivalence and infinite divisibility. *Journal of Applied Probability* **41**(02), 407–424.
- Reich, B. J. and Shaby, B. A. (2012) A hierarchical max-stable spatial model for extreme precipitation. *The annals of applied statistics* **6**(4), 1430.
- Røislien, J. and Omre, H. (2006) T-distributed random fields: A parametric model for heavy-tailed well-log data. *Mathematical Geology* **38**(7), 821–849.
- Rue, H., Martino, S. and Chopin, N. (2009) Approximate Bayesian inference for latent Gaussian models by using integrated nested Laplace approximations. *Journal of the royal statistical society (Series B)* **71**(2), 319–392.
- Sato, K.-I. (1999) *Lévy processes and infinitely divisible distributions*. Cambridge University Press.
- Seguro, J. V. and Lambert, T. W. (2000) Modern estimation of the parameters of the Weibull wind speed distribution for wind energy analysis. *Journal of Wind Engineering and Industrial Aerodynamics* **85**(1), 75–84.
- Simkova, L. (2017) *CharFun: Numerical Computation Cumulative Distribution Function and Probability Density Function from Characteristic Function*. R package version 0.1.0.
- Soubeyrand, S., Roques, L., Coville, J. and Fayard, J. (2011) Patchy patterns due to group dispersal.

- Journal of Theoretical Biology* **271**(1), 87–99.
- Stephenson, A. G. (2009) High-dimensional parametric modeling of multivariate extreme events. *Australian & New Zealand Journal of Statistics* **51**(1), 77–88.
- Stevens, M. J. M. and Smulders, P. T. (1979) The estimation of the parameters of the Weibull wind speed distribution for wind energy utilization purposes. *Wind engineering* **3**, 132–145.
- Strokorb, K., Ballani, F. and Schlather, M. (2015) Tail correlation functions of max-stable processes. *Extremes* **18**(2), 241–271.
- Varin, C., Reid, N. and Firth, D. (2011) An overview of composite likelihood methods. *Statistica Sinica* pp. 5–42.
- Varin, C. and Vidoni, P. (2005) A note on composite likelihood inference and model selection. *Biometrika* **92**(3), 519–528.
- Wadsworth, J., Tawn, J. A., Davison, A. and Elton, D. M. (2017) Modelling across extremal dependence classes. *Journal of the Royal Statistical Society (Series B)* **79**(1), 149–175.
- Wadsworth, J. L. and Tawn, J. A. (2012) Dependence modelling for spatial extremes. *Biometrika* **99**(2), 253–272.
- Wakefield, J. (2006) Disease mapping and spatial regression with count data. *Biostatistics* **8**(2), 158–183.
- Wang, J. and Genton, M. G. (2006) The multivariate skew-slash distribution. *Journal of Statistical Planning and Inference* **136**(1), 209–220.
- Watanabe, T. (2008) Convolution equivalence and distributions of random sums. *Probability Theory and Related Fields* **142**(3), 367–397.
- Wolpert, R. L. and Ickstadt, K. (1998a) Simulation of Lévy random fields. *Practical nonparametric and semiparametric Bayesian statistics* pp. 227–242.
- Wolpert, R. L. and Ickstadt, K. (1998b) Poisson/gamma random field models for spatial statistics. *Biometrika* **85**(2), 251–267.